Chalcogenide Letters Vol. 13, No. 6, June 2016, p. 281 - 289

ELASTIC PROPERTIES OF TeO_2-B_2O_3—ZnO-Gd_2O_3 GLASSES USING NON-DESTRUCTIVE ULTRASONIC TECHNIQUE

C. EEVON, M. K. HALIMAH[*], Z. AZMI, C. AZURAHANIM
Physics Department, Faculty of Science, University Putra Malaysia, 43400 UPM Serdang, Selangor, Malaysia

The addition of Gd_2O_3 causes the glass system to be highly ionic resulting in increasing rigidity and the tendency of devitrification. Gd_2O_3 affects the strength governing the elastic properties of the glass. The elastic moduli of the prepared glasses are expected to increase with the addition of the Gd_2O_3 due to increasing net molecular weight of prepared glass resulting in strong connectivity and more compactness of the glass network. The objective of this present work is to study the elastic properties of TeO_2-B_2O_3-ZnO doped Gd_2O_3 using a non-destructive ultrasonic technique. A series of $\{[(TeO_2)_{0.7}(B_2O_3)_{0.3}]_{0.7}(ZnO)_{0.3}\}_{1-x}(Gd_2O_3)_x$ glasses with x = 0.01, 0.02, 0.03, 0.04 and 0.05 mol were prepared by conventional melt-quenching method. Both longitudinal and shear ultrasonic velocities were measured using a pulse-echo method at a frequency of 5 MHz at room temperature. The elastic moduli (longitudinal modulus, shear modulus, Young's modulus and Bulk modulus), Poisson's ratio, Debye temperature, micro-hardness and softening temperature have also been quantified. The experimental results show that the elastic properties depend on the composition of the glass systems and the role of Gd_2O_3 inside the glass network.

(Received April 18, 2016; Accepted June June 22, 2016)

Keywords: Gadolinium ion; Zinc Borotellurite glass; Elastic moduli; Poisson's ratio; Debye temperature; Microhardness; Softening temperature

1. Introduction

Recently, there is an ongoing interest towards the fabrication of rare earth doped glasses due to a wide range of application such as in photonics, optoelectronics and sensors. They have unique properties such as high mechanical resistance, enhanced magnetic properties, higher chemical durability and photo-induced non-linear optical properties due to anharmonic electron-phonon interactions [1-4].

Rare earth oxide such as gadolinium oxide, Gd_2O_3 is a promising component material for photonics and optoelectronics application. The addition of Gd_2O_3 causes the glass system to be highly ionic which results in increasing rigidity and the tendency of devitrification of glass system [5-7]. It is interesting to evaluate how rare earth oxide such as Gd_2O_3 affects the strength governing the elastic constant of the glasses. So far, there is not much research on the elastic properties of zinc borotellurite glasses doped with gadolinium oxide, Gd_2O_3. The elastic properties of gadolinium zinc borotellurite glasses can be studied by measuring the ultrasonic velocities and densities of the glass samples. The ultrasonic velocities can be attained using a non-destructive ultrasonic technique. Ultrasonic technique is a technique used to study the structure of the glass that relate to the interatomic potentials [8]. Besides, this technique can also be used to examine the microstructure, characterization, mechanical properties, phase change and to evaluate elastic constants. In addition, the ultrasonic technique can also be used to characterize a different type of glasses or glass ceramics and to obtain information about the solid state motion in the material [9]. Hence, the objective of this present work is to study the elastic properties of TeO_2-B_2O_3-ZnO glasses doped with Gd_2O_3 using a non-destructive ultrasonic technique. The elastic moduli of the

---

[*] Corresponding author: hmk6360@gmail.com

prepared glasses are expected to increase with addition of the Gd_2O_3 due to increasing in the net molecular weight of the prepared glass that result in strong connectivity and increases compactness of the glass network

2. Experimental

Glass of $\{[(TeO_2)_{0.7}(B_2O_3)_{0.3}]_{0.7}(ZnO)_{0.3}\}_{1-x}(Gd_2O_3)_x$ with x = 0.01, 0.02, 0.03, 0.04 and 0.05 mol was prepared using a conventional melt-quenching method. Each component oxide used in the experiment was weighed using electronic beam balance with an uncertainty of ±0.0001 g and was mixed using mortar and pestle. The mixtures were transferred to furnace at 400^{o}C for drying followed by another furnace for melting. The melted molten was poured into cylindrical shape mould that was preheated during melting and was transferred back into the furnace for annealing. The samples obtained were cut into the thickness of 5mm each and were polished using sandpaper to obtain parallel surfaces on both sides. The excessive glass samples were crush into powder form for structural analysis. Structural analysis of the prepared samples was studied using X-ray diffraction (XRD) analysis. The density, ρ, of the glasses was measured using electronic densimeter MD-300S based on Archimedes' principle and the molar volume, V_m, was calculated. Ultrasonic velocities of the prepared glasses were obtained using a pulse-echo method. The pulse passes through the specimen that is bonded to the transducer and an echo is recorded each time and returns to the transducer. The ultrasonic wave velocity can be calculated using $v = 2d/\Delta t$ where d is the sample thickness and Δt is the time interval between two consecutive echoes. Both longitudinal and shear ultrasonic measurements were carried out by using MATEC 1C7-5R M049 and OLYMPUS V155 respectively. All measurements were taken at a frequency of 5 MHz at room temperature. The ultrasonic velocities and densities obtained can be used for determination of elastic moduli (Longitudinal modulus, L, Shear modulus, S, Bulk modulus, K and Young's modulus, E) and Poisson's ratio, σ, using the following relations [8]:

$$L = \rho v_L^2 \tag{1}$$

$$G = \rho v_s^2 \tag{2}$$

$$K = L - (4/3)G \tag{3}$$

$$E = 2(1 + \sigma)G \tag{4}$$

$$\sigma = (L - 2G)/2(L - G) \tag{5}$$

where v_L and v_s are ultrasonic longitudinal and shear velocities respectively.
Microhardness, H, Debye temperature, θ_D and softening temperature, T_S were calculated from the following equation as reported in [8]:

$$H=\frac{(1-2\sigma)E}{6(1+\sigma)} \tag{6}$$

$$T_S=\left(\frac{Mv_s^2}{c^2n}\right) \tag{7}$$

where M is the molecular weight of the glass, c is constant equal to 0.5074 x 10^5 cms^{-1}K$^{-1/2}$ and n is the number of atoms.

$$\theta_D=\frac{h}{k}\left(\frac{3\varphi N_A}{4\pi V_M}\right)^{\frac{1}{3}}U_m \tag{8}$$

where h is Planck's constant, k is Boltzmann's constant, N_A is Avogadro's number, V_M is molar volume, φ is the number of atoms in the chemical formula and U_m is the mean ultrasonic velocity defined by:

$$U_m=[\frac{1}{3}\left(\frac{1}{v_L{}^3}+\frac{2}{v_s{}^3}\right)]^{-\frac{1}{3}} \quad (9)$$

3. Results and Discussion

3.1 X-ray diffraction analysis

The XRD pattern of $\{[(TeO_2)_{0.7}(B_2O_3)_{0.3}]_{0.7}(ZnO)_{0.3}\}_{1-x}(Gd_2O_3)_x$ are shown in Figure 1. The XRD pattern of the present glass does not shows any distinguishable sharp peaks but shows broad hump at a low angle which shows the characteristic of amorphous materials. This result is in agreement with the previous work done by Halimah et al. and Azlan et al. [8,10].

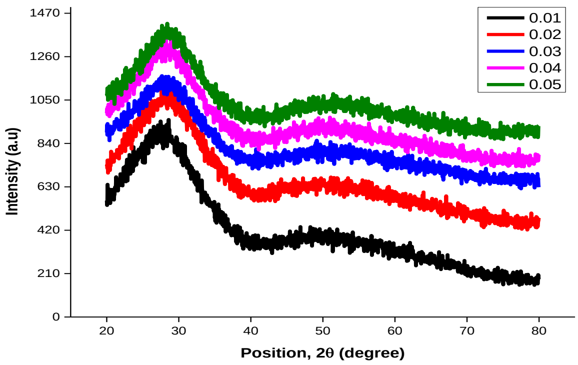

Fig 1. XRD pattern of $\{[(TeO_2)_{0.7}(B_2O_3)_{0.3}]_{0.7}(ZnO)_{0.3}\}_{1-x}(Gd_2O_3)_x$ *Glasses*

3.2 Density and Molar Volume

The variation of density, molar volume and oxygen molar volume of $\{[(TeO_2)_{0.7}(B_2O_3)_{0.3}]_{0.7}(ZnO)_{0.3}\}_{1-x}(Gd_2O_3)_x$ glasses are tabulated in Table 1. Figure 2 shows the variation of density and molar volume. The density of the prepared glasses increases from 4500 to 4897 ± 10 kg/m^3 as the concentration of Gd_2O_3 increases from 1.0 to 5.0 mol%. The increase in density of the prepared glass is due to the substitution of lower molecular weight ZnO-TeO_2-B_2O_3 (310.5984 g/mol) with higher molecular weight Gd_2O_3 (362.4982 g/mol) which in turn, an increase in the overall average molecular weight. This result in stronger connectivity in the glass network and hence increase in density [11, 12].

The molar volume, V_m of the present glass is calculated using,

$$V_m=\frac{M}{\rho} \quad (10)$$

where M is the molecular weight of the glass sample and ρ is the density of glass [13]. The molar volume decreases from 2.660 x 10^{-5} to 2.613 x 10^{-5} ±0.01 m^3/mol as the concentration of Gd_2O_3 increases from 1.0 to 3.0 mol% and increases from 2.613x 10^{-5} to 2.645x 10^{-5} ±0.01 m^3/mol as the concentration of Gd_2O_3 increases from 3.0 to 5.0 mol% The density and molar volume show opposite behavior as shown by the relation $V_m=\frac{M}{\rho}$. When density increases, the molar volume decreases. The decrease in molar volume is due to lower in the total number of oxygen atoms that causes the glass network to become tightly packed [2]. The decrease in oxygen molar volume as shown in Figure 3 also contributed to the decrease in molar volume of the glasses. The decrease in oxygen molar volume shows that there is a decrease in formation of non-bridging oxygen (NBO) atoms. Hence, the decrease in molar volume indicates the decreasing of free space in the glass network [14, 15]. However, at x = 0.03 mol, the density and molar volume increases as the concentration of Gd_2O_3 increases. This is due to large effective ionic radius of Gd^{3+} ions (r = 93.8

pm) as compared to Te^{4+} ions (r = 50pm) and B^{3+} (r = 12pm). The further increase of Gd^{3+} ions in the glass network results in the formation of excess free volume which is due to the difference between the effective ionic radius between Gd^{3+}, Te^{4+} and B^{3+} ions [23]. The increase in glass molar volume shows that the rigid network structure become more open.

Table 1: Density, molar volume and oxygen molar volume of $\{[(TeO_2)_{0.7}(B_2O_3)_{0.3}]_{0.7}(ZnO)_{0.3}\}_{1-x}(Gd_2O_3)_x$ Glasses

Mole, x	ρ (kg/m^3)	V_m (x10^{-5}m^3/mol)	V_o (x10^{-5} m^3/mol)
0.01	4500	2.660	1.385
0.02	4672	2.615	1.353
0.03	4769	2.613	1.345
0.04	4850	2.620	1.341
0.05	4897	2.645	1.346

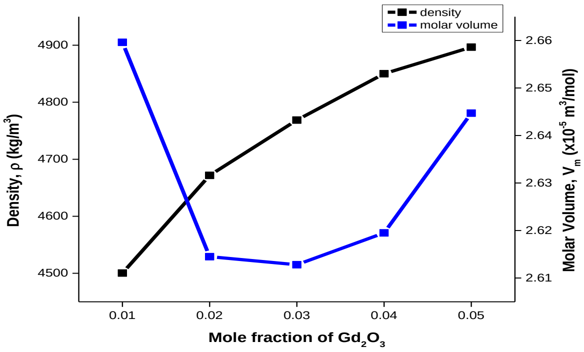

Fig. 2. Density and molar volume of $\{[(TeO_2)_{0.7}(B_2O_3)_{0.3}]_{0.7}(ZnO)_{0.3}\}_{1-x}(Gd_2O_3)_x$ Glasses

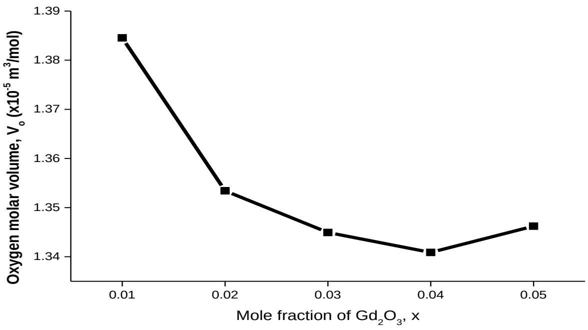

Fig. 3. Oxygen molar volume of $\{[(TeO_2)_{0.7}(B_2O_3)_{0.3}]_{0.7}(ZnO)_{0.3}\}_{1-x}(Gd_2O_3)_x$ Glasses

3.3 Elastic Properties

The variation of longitudinal and shear ultrasonic velocities of $\{[(TeO_2)_{0.7}(B_2O_3)_{0.3}]_{0.7}(ZnO)_{0.3}\}_{1-x}(Gd_2O_3)_x$ glasses at room temperature is listed in Table 2 and is shown in Figure 4.

Table 2. Ultrasonic velocities (Longitudinal and shear ultrasonic velocity) and elastic moduli (longitudinal, shear, Young's and bulk modulus) of $\{[(TeO_2)_{0.7}(B_2O_3)_{0.3}]_{0.7}(ZnO)_{0.3}\}_{1-x}(Gd_2O_3)_x$ *Glasses*

v_L (m/s)	v_s (m/s)	L (GPa)	G (GPa)	E (GPa)	K (GPa)
3936	2222	69.71	22.23	56.28	40.07
4002	2244	74.82	23.52	57.29	43.45
3960	2177	74.78	22.59	57.28	44.66
4035	2217	78.98	23.84	57.98	47.19
4076	2259	81.35	25.00	58.33	48.02

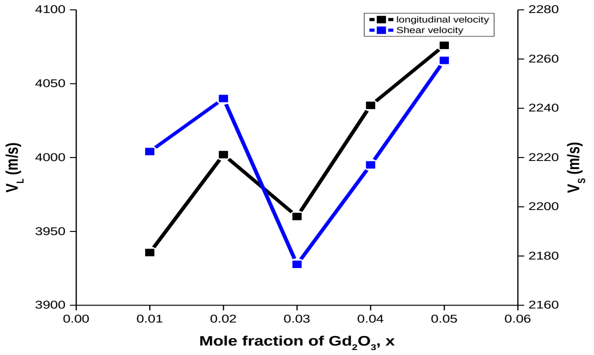

Fig. 4. Ultrasonic velocities of $\{[(TeO_2)_{0.7}(B_2O_3)_{0.3}]_{0.7}(ZnO)_{0.3}\}_{1-x}(Gd_2O_3)_x$ *Glasses*

The longitudinal ultrasonic velocity increases from 3935 to 4076 m/s and shear ultrasonic velocity increases from 2222 to 2259 m/s. However, at x = 0.02 mol, both the longitudinal and shear ultrasonic velocities start to decrease to x = 0.03 mol. There is a significant change in glass structure after addition of Gd_2O_3 due to the difference in the ultrasonic velocities of the glass network [16]. It is observed that both velocities start to increase from x = 0.03 to 0.05 mol. The increase in the ultrasonic velocities is related to increase in rigidity of the glass. The addition of Gd_2O_3 into the ternary zinc borotellurite glasses results in a change of structural units from TeO_3 to TeO_4 with the formation of bridging oxygen atoms (BOs) which cause the glass network to become tightly packed [8]. The increase in longitudinal and shear ultrasonic velocities is also due to the decrease in oxygen molar volume which results in strengthening of glass structure [17].

In the presently studied glasses, the elastic moduli obtained from the equation (1-5) are tabulated in Table 2 and shown in Figure 5.

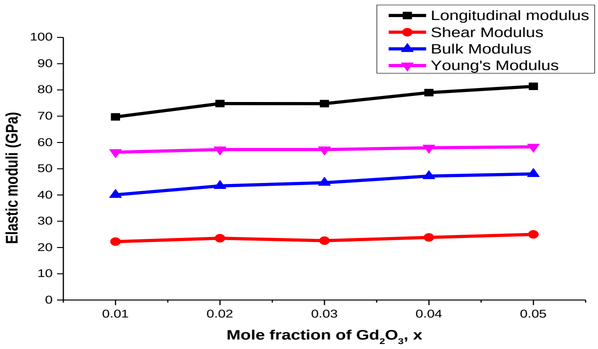

Fig. 5: Elastic moduli of $\{[(TeO_2)_{0.7}(B_2O_3)_{0.3}]_{0.7}(ZnO)_{0.3}\}_{1-x}(Gd_2O_3)_x$ *Glasses*

The longitudinal modulus, L, ranged from 69.71 to 81.35 GPa, shear modulus, G, from 22.23 to 25.00 GPa, bulk modulus, K, from 40.07 to 48.02 GPa and Young's modulus, E, from 56.28 to 58.33 GPa. The increase in the elastic moduli of the prepared glasses can be attributed to the change in the structural unit of the glass from TeO_3 to TeO_4 with the formation of bridging oxygen atoms. The increase in the rigidity of the glass is attributed to the increase of elastic moduli of the glass samples [8, 18]. The large differences observed between longitudinal modulus, L, and shear modulus, G, arises from the effect of volume. The change in volume is due to compressions and expansions which involved in longitudinal strain are clearly shown whereas there is no change in volume in shear strain [19].

Poisson's ratio is defined as the ratio of lateral and longitudinal strain produced when a tensile force is applied. Figure 6 shows the variation of Poisson's ratio.

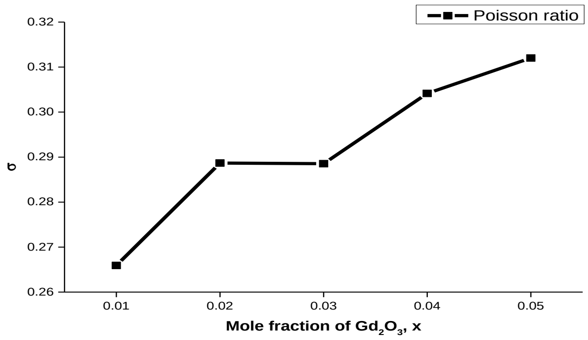

Fig. 6. Poisson's ratio of $\{[(TeO_2)_{0.7}(B_2O_3)_{0.3}]_{0.7}(ZnO)_{0.3}\}_{1-x}(Gd_2O_3)_x$ *Glasses*

The value of Poisson's ratio increases from 0.27 to 0.31 as the concentration of Gd_2O_3 increases from 0.01 to 0.05 mol. The values of Poisson's ratio are affected by the changes in crosslink density which indicates that the structure of the prepared glasses has high cross-link density [16]. The increase in Poisson's ratio can also be attributed to the change in the type of bonding from covalent bonds to ionic bonds [20]. Another factor that affects Poisson's ratio is the increase in the average cross-link density of the glass [14].

Microhardness is the pressure required to eliminate the free volume in glass and indicates the deformation of the glass network. The free volume of the glass decreases due to high hydrostatic pressure which results in compactness of glass. Debye temperature is used to determine the elastic moduli and atomic vibrations at which all the low frequency lattice vibrational modes are excited. Softening temperature is used to determine the temperature stability of the glass [8-9, 20-21].

Thermal expansion coefficient, α_p, can be obtained using,

$$\alpha_p=23.2(v_L-0.57457) \tag{11}$$

where v_L is ultrasonic longitudinal velocity of the glasses.

The values of microhardness, Debye temperature, softening temperature and thermal expansion coefficient obtained are tabulated in Table 3 and shown in Fig. 7 to 10 respectively. The values of microhardness decrease from 3.469 to 2.786 GPa as the concentration of Gd_2O_3 content increases from 0.01 to 0.05 mol. The decrease in microhardness, H, might due to change of structural units from TeO_3 to TeO_4 with the formation of bridging oxygen atoms that results in increasing of compactness of the glass network. Debye temperature and the softening temperature generally increase from 305 to 313 K and 731.6 to 798.9 K respectively, as the concentration of Gd_2O_3 increases from 0.01 to 0.05 mol. The main reason for this is the increase in the number of atoms in the chemical formula and ultrasonic velocities of glass. The increase in Debye temperature, softening temperature and thermal expansion coefficient indicates the strengthening of the glass due to the formation of bridging oxygen [22].

Table 3. Poisson's ratio, microhardness, Debye temperature, softening temperature and thermal expansion coefficient of $\{[(TeO_2)_{0.7}(B_2O_3)_{0.3}]_{0.7}(ZnO)_{0.3}\}_{1-x}(Gd_2O_3)_x$ *Glasses*

Mole, x	σ	H (GPa)	Θ_D (K)	T_s (K)	α_p (K^{-1})
0.01	0.27	3.469	305	731.6	91294.3
0.02	0.29	3.132	310	756.6	92831.8
0.03	0.29	3.134	302	721.8	91860.6
0.04	0.30	2.902	308	759.1	93605.4
0.05	0.31	2.786	313	798.9	94548.2

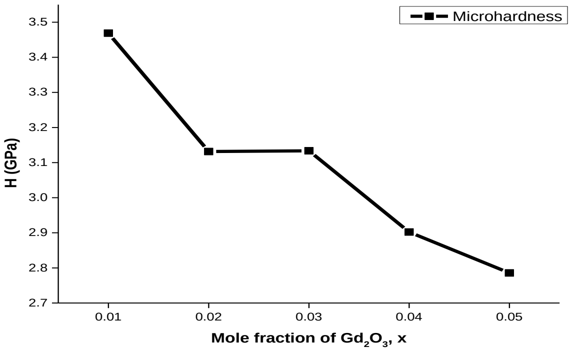

Fig. 7. Microhardness of $\{[(TeO_2)_{0.7}(B_2O_3)_{0.3}]_{0.7}(ZnO)_{0.3}\}_{1-x}(Gd_2O_3)_x$ *Glasses*

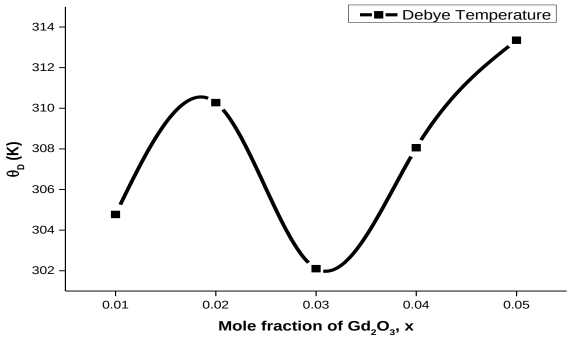

Fig. 8. Debye temperature of $\{[(TeO_2)_{0.7}(B_2O_3)_{0.3}]_{0.7}(ZnO)_{0.3}\}_{1-x}(Gd_2O_3)_x$ *Glasses*

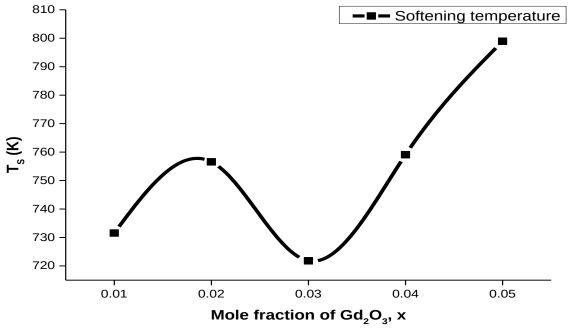

Fig. 9. Softening temperature of $\{[(TeO_2)_{0.7}(B_2O_3)_{0.3}]_{0.7}(ZnO)_{0.3}\}_{1-x}(Gd_2O_3)_x$ *Glasses*

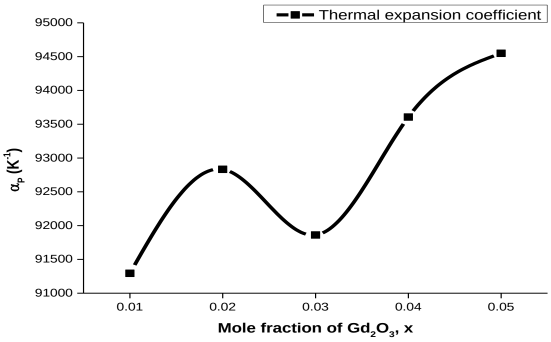

Fig. 10. Thermal expansion coefficient of $\{[(TeO_2)_{0.7}(B_2O_3)_{0.3}]_{0.7}(ZnO)_{0.3}\}_{1-x}(Gd_2O_3)_x$ *Glasses*

4. Conclusion

Quaternary zinc borotellurite with composition $\{[(TeO_2)_{0.7}(B_2O_3)_{0.3}]_{0.7}(ZnO)_{0.3}\}_{1-x}(Gd_2O_3)_x$, x = 0.01, 0.02, 0.03, 0.04 and 0.05 mol, has been successfully prepared. The characteristics of gadolinium zinc borotellurite glasses were studied thoroughly. XRD patterns show that the present glasses were amorphous in nature. The density of gadolinium zinc borotellurite glasses increases as Gd_2O_3 content increases while molar volume shows both decreasing and increasing values. The changes in density and molar volume are due to the high molecular weight of Gd_2O_3 and structural change in the glass network. The observed change in ultrasonic velocities shows that there is a substantial change in the glass structure. The increase in ultrasonic velocities is due to the increase in rigidity of glass and change in structural units. Elastic moduli and other parameters were achieved and show that there is an increase in the rigidity of the glass.

Acknowledgments

The authors appreciate the financial support for the work from Universiti Putra Malaysia through GPIBT (9411800).

References

[1] H. Luo, X. Hu, W. Liu, Y. Zhang, A. Lu, X. Hao, Journal of Non-Crystalline Solids **389**, 86 (2014).
[2] X. Liang, H. Li, C. Wang, H. Yu, Z. Li, S. Yang, Journal of Non-Crystalline Solids, **402**, 135 (2014).
[3] Y. B. Saddeek, I. S. Yahia, K. A. Aly, W. Dobrowolski, Solid State Sciences, **12**(8), 1426 (2010).
[4] T. Ristoiu, E. Culea, I. Bratu, Materials Letters, **41**(3), 135 (1999).
[5] N. Elkhoshkhany, R. Abbas, R. El-Mallawany, A. J. Fraih, Ceramics International, **40**(9), 14477 (2014).
[6] N. Elkhoshkhany, R. Abbas, R. El-Mallawany, K. S. H. HumoudSharba, Ceramics International, **40**(8), 11985 (2014).
[7] N. Elkhoshkhany, R. Abbas, M. S. Gaafar, R. El-Mallawany, Ceramics International. (2015).
[8] M. K. Halimah, W. M. Daud, H. A.A. Sidek, Ionics, **16**(9), 807. (2010).
[9] A.N. Kannappan, S. Thirumaran, R. Palani, ARPN Journal of Engineering and Applied Sciences, **4**(1), 27 (2009).
[10] M. N. Azlan, M. K. Halimah, S. Z. Shafinas, W. M. Daud, Chalcogenide Letters, **11**(7), 319 (2014).
[11] P. Gayathri Pavani, K. Sadhana, V. Chandra Mouli, Physica B: Condensed Matter, **406**(6-7), 1242 (2011).

[12] H. Luo, X. Hu, W. Liu, Y. Zhang, A. Lu, X. Hao, Journal of Non-Crystalline Solids, **389**, 86 (2014).
[13] R. S. Kundu, S. Dhankhar, R. Punia, K. Nanda, N. Kishore, Journal of Alloys and Compounds, **587**, 66 (2014).
[14] M. S. Gaafar, I. Shaarany, T. Alharbi, Journal of Alloys and Compounds, **616**, 625 (2014).
[15] V. C. Veeranna Gowda, Physica B: Condensed Matter, **456**, 298 (2015).
[16] Y. B. Saddeek, Materials Chemistry and Physics, **91**(1), 146 (2005).
[17] Y. B. Saddeek, L. A. El. Latif, PhysicaB*:* Condensed Matter, **348**, 475 (2004).
[18] E. S. Yousef, A. El-Adawy, N. El-KheshKhany, Solid State Communications, **139**(3), 108 (2006).
[19] R. El-Mallawany, N. El-Khoshkhany, H. Afifi, Materials Chemistry and Physics, **95**(2-3), 321 (2006).
[20] M. S. Gaafar, N. S. A. El-Aal, O. W. Gerges, G. El-Amir, Journal of Alloys and Compounds, **475**(1-2), 535 (2009).
[21] Y. B. Saddeek, Materials Chemistry and Physics, **83**(2-3), 222 (2004).
[22] M.K. Halimah, H.A.A. Sidek, W.M. Daud, H. Zainul, Z. A. Talib, A. W. Zaidan, A. S. Zainal, H. Mansor, American Journal of Applied Sciences, **2**(11), 1541 (2005).
[23] S. S. Hajer, M. K. Halimah, Z. Azmi, M. N. Azlan, Chalcogenide Letters, **11**(11), 553 (2014).